Photosynthesis Research (2021) 150:179–193
https://doi.org/10.1007/s11120-020-00812-0

ORIGINAL ARTICLE

The different patterns of post-heat stress responses in wheat genotypes: the role of the transthylakoid proton gradient in efficient recovery of leaf photosynthetic capacity

Erik Chovancek[1] · Marek Zivcak[1] · Marian Brestic[1] · Sajad Hussain[2,3] · Suleyman I. Allakhverdiev[4]

Received: 6 July 2020 / Accepted: 8 December 2020 / Published online: 3 January 2021

Abstract

The frequency and severity of heat waves are expected to increase in the near future, with a significant impact on physiological functions and yield of crop plants. In this study, we assessed the residual post-heat stress effects on photosynthetic responses of six diverse winter wheat (*Triticum* sp.) genotypes, differing in country of origin, taxonomy and ploidy (tetraploids vs. hexaploids). After 5 days of elevated temperatures (up to 38 °C), the photosynthetic parameters recorded on the first day of recovery (R1) as well as after the next 4–5 days of the recovery (R2) were compared to those of the control plants (*C*) grown under moderate temperatures. Based on the values of CO_2 assimilation rate (*A*) and the maximum rates of carboxylation (V_{Cmax}) in R1, we identified that the hexaploid (HEX) and tetraploid (TET) species clearly differed in the strength of their response to heat stress. Next, the analyses of gas exchange, simultaneous measurements of PSI and PSII photochemistry and the measurements of electrochromic bandshift (ECS) have consistently shown that photosynthetic and photoprotective functions in leaves of TET genotypes were almost fully recovered in R2, whereas the recovery of photosynthetic and photoprotective functions in the HEX group in R2 was still rather low. A poor recovery was associated with an overly reduced acceptor side of photosystem I as well as high values of the electric membrane potential ($\Delta\psi$ component of the proton motive force, *pmf*) in the chloroplast. On the other hand, a good recovery of photosynthetic capacity and photoprotective functions was clearly associated with an enhanced ΔpH component of the *pmf*, thus demonstrating a key role of efficient regulation of proton transport to ensure buildup of the transthylakoid proton gradient needed for photosynthesis restoration after high-temperature episodes.

Keywords Wheat · Heat stress · Recovery · Electrochromic bandshift · Proton transport · Ploidy

Introduction

Heat stress is one of the most important abiotic stressors limiting the growth of crop plants in large production areas worldwide, leading to drastic losses in the yield and quality of these crops. Therefore, a tolerance to heat stress is highly desirable, and searching for the appropriate traits or genes is

Erik Chovancek and Marek Zivcak made an equal contribution to this work.

Supplementary Information The online version of this article (https://doi.org/10.1007/s11120-020-00812-0) contains supplementary material, which is available to authorized users.

✉ Marek Zivcak
marek.zivcak@uniag.sk

✉ Suleyman I. Allakhverdiev
suleyman.allakhverdiev@gmail.com

[1] Department of Plant Physiology, Slovak University of Agriculture, Nitra, Slovak Republic

[2] College of Agronomy, Sichuan Agricultural University, Chengdu, People's Republic of China

[3] Sichuan Engineering Research Center for Crop Strip Intercropping System, Key Laboratory of Crop Ecophysiology and Farming System in Southwest China, Sichuan Agricultural University, Chengdu, People's Republic of China

[4] K.A. Timiryazev Institute of Plant Physiology, Russian Academy of Sciences, Moscow, Russia

an integral part of numerous breeding programs (Driedonks et al. 2016).

Numerous examples show the diversity of photosynthetic responses of different crop genetic resources to high temperature (Hede et al. 1999; Stefanov et al. 2011; Brestic et al. 2012). If the plants are subjected to elevated nonlethal temperatures (heat acclimation), they can acquire protection from the later influence of heat (Vegh et al. 2018), but the acclimation capacity varies among genotypes (Brestic et al. 2012) or ecotypes (Psidova et al. 2018). Most of the screening studies focus on very simple photosynthesis-related parameters such as the chlorophyll content or chlorophyll fluorescence parameters in leaves in plants during and after exposure to high temperature or investigate the thermostability of the photosynthetic complexes in response to elevated temperature levels. Much attention has also been paid to the changes in photosynthetic enzyme activities and the photosystem II activity and damage (Singh et al. 2007; Allakhverdiev et al. 2008). On the other hand, much less attention has been paid to the screening of genotype-related differences in proton transport and the kinetic forces created on the thylakoid membrane that drive photosynthesis and their possible changes in response to heat effects and recovery.

ATP synthesis in chloroplasts, which takes place on CF_0-CF_1-type ATP synthase, is driven by the thylakoid proton motive force (*pmf*). The *pmf* is unequally composed of two components, a proton concentration difference (ΔpH) and an electric potential (Δψ). Furthermore, the *pmf* acts as a key regulator in mechanisms of photoprotection by reflecting the energy level and the physiological fitness of the chloroplast (Davis et al. 2017; Cruz et al. 2005). The pmf is thus a key regulatory mechanism for optimizing the tradeoff between ATP synthesis and photoprotection.

The proton gradient ΔpH is generated by the release of protons from the oxygen-evolving complex (OEC) of photosystem II (PSII) in the process of water oxidation and by the transfer of protons when plastoquinone (PQ) is reduced and reoxidized in the electron transfer mechanism (Kanazawa et al. 2017; Avenson et al. 2004). In turn, this proton gradient is depleted by the activity of ATP synthase. As a result, the pH in lumen ranges from 5.5 to 7.5 (Vinyard and Brudvig 2017). Low pH triggers (through activation of violaxanthin deepoxidase and protonation of PsbS, a protein in PSII) the processes of energy-dependent nonphotochemical quenching (qE), photoprotective mechanisms that impede overexcitation of PSII and thus inhibit the creation of harmful $^1O_2$. When the lumen becomes increasingly acidified, the rate of oxidation of plastoquinol decreases, electron transfer to cytochrome b6f and further in the chain decreases and the photosystem I (PSI) electron acceptors are protected from the accumulation of electrons (Kanazawa et al. 2017; Takizawa et al. 2007a). This process happens at the expense of the linear electron flow (LEF) (Avenson et al. 2005). However, under optimal conditions, the majority of protons are transported by ATP synthase into the stroma, and pH is buffered to prevent unwanted photoprotection. The formation of the electric potential Δψ depends on the following: (i) abovementioned H^+ proton gradient (positive charge in lumen), (ii) electrons in the photosynthetic electron transport, and (iii) movement of ions through `counter` ion channels (Cruz et al. 2001), which include a thylakoid potassium channel (Carraretto et al. 2013), a K^+/H^+ antiporter (Armbruster et al. 2014), and transporters for other charged species (Duan et al. 2016; Herdean et al. 2016a, b; Kunz et al. 2014; Schneider et al. 2016). Counterion flow, which represents pumping cations from lumen to stroma, results in the dissipation of Δψ, which slows ATP synthase activity, making protons accumulate in the lumen and resulting in qE activation.

The electron and proton transports are generally very efficient. However, oxidative photodamage occurs when the light harvesting rate is higher than the capacity to incorporate the harvested energy into chemical bonds. This process very often happens in high light but also under environmental conditions that are out of the optimum for the plant. Under these conditions, reactive intermediates can accumulate in the photosynthetic apparatus, leading to generation of reactive oxygen species (ROS), mainly $O_2^{-\circ}$ in PSI and mainly $^1O_2$ in PSII (Davis et al. 2017).

Nonlethal heat stress is known to arouse a whole set of processes in plants to avoid or decrease damage on the cellular level. To acclimate to heat, plants can (i) induce their antioxidative systems that effectively scavenge ROS and prevent membrane lipid peroxidation (Xu et al. 2006; Vegh et al. 2018; Kreslavski et al. 2009), (ii) synthesize heat shock proteins and osmoprotectants that stabilize the functional structures of the cell (Hasanuzzaman et al. 2013), (iii) adjust their signaling and gene expression (Almeselmani et al. 2006), and (iv) optimize energy distribution between two photosystems via state transitions (Nellaepalli et al. 2011) during long-term heat stress.

Wheat (*Triticum* sp. L.), an old and widespread crop species, has extremely rich germplasm characterized by an enormous phenotypic and genetic diversity. The collections of Genebanks contain an immense number of accessions belonging to modern wheat genotypes, landraces, and breeding lines as well as the wild ancestors of wheat assigned to various taxons, differing in ploidy and geographic distribution (Snook et al. 2011). The expected diversity of photosynthetic responses to high temperature in the wheat genotypes differing in taxonomy or provenance of origin was confirmed by our previous results focused specifically on diffusion limitations and PSII thermostability (Brestic et al. 2018) and regulation of electron transport under conditions of high temperature and beyond (Brestic et al. 2016; Chovancek et al. 2019).

In this study, we put a specific focus on the recovery of photosynthetic capacity and functions after a simulated heat wave in a diverse collection of wheat genotypes differing in taxonomy, ploidy, geographic origin and phenotype. Based on the gas exchange measurements, we identified two separate groups of genotypes differing in photosynthesis recovery patterns after the cessation of heat stress. In these two groups, we analyzed the processes related to the regulation of photosynthetic electron and proton transport, specifically targeting the links between the partitioning of two major components of the proton motive force and the overall photosynthetic capacity in a recovery phase.

Materials and methods

Cultivation of plants

Six varieties of winter wheat (*Triticum* sp.) were used in this study, of which 3 were hexaploid (HEX; $2n = 42$) bread wheat (*T. aestivum* L., cv. Thesee (France), SLO-16/26 (Slovenia), GRC-867 (Greece)) and 3 were tetraploid (TET; $2n = 28$) species (*T. durum* Desf., cv. Dušan (Serbia); *T. turgidum* L., cv. Unmedpur Mummy (India); *T. timopheevi* Zhuk., cv. AZESVK2009-90). The seeds were provided by the Genebank of NFFC-RIPP in Piešťany (Slovakia), and the genotypes were carefully selected from a larger collection tested in previous seasons within the phenotyping program at SUA Nitra. The 6 genotypes had a very similar phenological pattern, but they differed in phenotypic traits, as well as responses to water deficit. The experiment was established indoors during the winter period. After several days at room temperature, the seedlings were vernalized in a growth chamber at 5 °C with a photoperiod of 12/12 h (light/dark) for ~ 80 days. In spring, the plants were transplanted into pots (one plant per standard 3 L phenotyping pot) with a commercial peat substrate (Klassman-TS3) and Osmocote fertilizer (5 g). The pots were placed in the cultivation cage of the Slovak University of Agriculture in Nitra, Slovakia, exposing the plants to outdoor conditions with natural sunlight and temperature conditions. The plants were irrigated regularly to avoid dehydration. For the experiment, the pots were organized in a block surrounded by border plants to eliminate the border effect. The heat stress simulation was commenced when all plants were in a stage with developed spikes and flag leaves (the preanthesis period).

Heat stress simulation and scheduling of measurements

The heat stress was simulated by exposing plants for 4–6 days in a PE transparent foil tunnel with a high-light transmission. Inside the tunnel, the temperatures were 6–8 °C higher during the day and 2–3 °C higher at nighttime than the outdoor conditions. The maximum daily temperature in the tunnel in terms of individual days ranged from 33–38 °C, whereas the maximum temperature outdoor was 25–31 °C. All measurements presented in this study were realized under laboratory conditions at ~ 25 °C. On the 5th to 7th day, the plants were removed from the tunnel for measurements of photosynthetic and other parameters. These plants were labeled R1 and represented an early recovery (the plants were exposed to a moderate temperature level for at least 12 h). Then, 3–5 days after cessation of heat stress, the measurements of the R2 recovery period were realized. The controls (C) were measured one day before or after the stress measurements. The simultaneous measurements of PSI and PSII, the gas exchange measurements and electrochromic bandshift (ECS) measurements were obtained under laboratory conditions. In all genotypes, the measurements were performed on the youngest, fully expanded leaf (the flag leaf of wheat). Because of the very time-consuming measuring protocols applied and the high number of genotypes, only 3 plants of each genotype and variant were analyzed. A random sequence of measurements was applied with a substantial light recovery period between measuring the same leaves using different devices.

Heat acclimation estimation

To assess the impact of heat on individual leaf gas exchange parameters (Y), the heat acclimation index (HAI) was calculated as $\mathrm{HAI} = Y_{\mathrm{R1}}/Y_{\mathrm{C}}$ (Silim et al. 2010; Perdomo et al. 2016). To compare heat responses of different varieties of wheat, graphical expressions of slopes of changes in the V_{Cmax} parameter were used (Suppl. Fig. 3).

Gas exchange measurements

To estimate the gas exchange parameters, we applied an A/C_i curve protocol using an Li-6400XT gasometer (Licor, USA). The samples were exposed to 1500 µmol photons m^{-2} s^{-1}, with a leaf temperature of 25 °C, and ambient air humidity. First, steady-state photosynthesis was reached in the sample inside the gasometer chamber head. Then, the CO_2 response curve was applied by a stepwise change in the CO_2 level: 400, 300, 250, 200, 150, 100, 50, 400, 600, 800, 1000, 1200, and 1500 ppm. The values of gas exchange parameters (photosynthesis rate—A; stomatal conductance—g_s; internal CO_2 concentration—c_i) were calculated directly by the gas analyzer software. The maximum carboxylation rate, V_{Cmax}, and the maximum electron transport rate, J_{max}, were determined by analysis of A/C_i curves (representatives in Supl. Fig. 1) according to the model of Farquhar–von Caemmerer–Berry (Farquhar et al. 1980) edited by Ethier and Livingston (Ethier 2004) acquired from http://landflux.org. $\mathrm{ETR_{PSII}}$ was calculated

from the values of PSII quantum yield and light intensity, assuming the equal absorbance (0.84) and equal distribution of absorbed light between two photosystems as: $ETR_{PSII} = 0.84*0.5*$ Y(II) *PAR (Baker 2008).

Measurements of electrochromic bandshift

Measurements of electrochromic bandshift (ECS) were performed with a LED-based spectrophotometer (JTS 10, Biologic, France) following Zivcak et al. (Zivcak et al. 2014). First, a single turnover was determined by applying a saturating pulse on the sample. Then, after applying an actinic light with an intensity of ~ 900 µmol photons m^{-2} s^{-1} for 7 min, the measurement of ECS decay at 520 nm took place during 30 s of darkness. Then, light was turned on for the next 2–3 min, and the ECS decay at 546 nm was measured on the same place of the leaf. White LED filtered at 520 and 546 nm provided the measuring flashes. The 546 nm signal was subtracted from 520 nm signal, i.e., I_{520}–I_{546}, to calculate the ECS parameters. In this way, the contribution of redox changes related to electron transport were deconvoluted from the signal (example shown in Supl. Fig. 2). The analysis of ECS decay was performed according to the DIRK (dark interval relaxation kinetics) ECS analysis pipeline (Sacksteder et al. 2000). By analysis of the ECS decay, we determined the magnitude of proton conductivity of ATP synthase, g_H^+, and the amplitude of the ECS signal (ESC_t). The ECS_t is assumed from the difference in steady-state ECS signals in light before the light was switched off and the minimum value of the ECS signal, observed after ~ 150 ms of the dark period. The inverse of the first-order decay time of ECS toward a quasistable state is rendered as g_H^+ (Baker et al. 2007).

Simultaneous measurements of PSII and PSI photochemistry

The state of PSII and PSI photochemistry was measured with a Dual PAM-100 system (Walz, Germany) with a ChlF unit and P700 dual wavelength (830/875 nm) unit, as described in Chovancek et al. (2019). The basic parameters used for calculations were measured in dark adapted samples, in steady state, after photosynthesis had been induced, and during rising intensities of irradiance, i.e., so-called light response curves. The ChlF and P700 parameters were calculated using the formulae of Klughammer and Schreiber (1994).

Data processing and statistical analysis

The data were subjected to statistical assessment using ANOVA (STATISTICA 10, StatSoft, Tulsa, USA), followed by the post hoc comparison of the mean values using Duncan test. In most of the graphs, the mean values ± standard errors are presented. The measurements were performed on at least 3 plants of each of the six varieties. The graphs are based on the results of these statistical analysis.

Results

CO_2 assimilation and photosynthetic limitations in recovery after prolonged heat stress

Comparison of the values of the CO_2 assimilation rate (A) in individual genotypes measured in the early stage of recovery (R1) indicated a decrease in the photosynthetic rate compared to that in the control plants (Fig. 1a). However, a significant decrease was observed in 3 genotypes only (AZE, UMY, DUS). To eliminate diffusion (mostly stomatal) limitations, we also compared the maximum carboxylation rate, V_{Cmax} (Fig. 1b), derived from the A/C_i curves (representatives in Supl. Fig. 1). Obviously, the decrease in V_{Cmax} is insignificant and mostly negligible in the hexaploid (HEX) bread wheat cultivars (THE, 16/26, GR8), whereas in the tetraploid (TET) genotypes, we observed a highly significant decrease in V_{Cmax}.

Thus, the maximum carboxylation rate, V_{Cmax}, decreased in HEX plants by only 12%, whereas the value decreased in the TET group by 56% (Fig. 2b) on average. The results shown in Fig. 1b, as well as the slope of the decrease in V_{Cmax} (Supl. Fig. 3), clearly indicate that the two groups showed different responses to the prolonged heat stress period. Along with V_{Cmax}, the maximum electron transport rate, J_{max}, also decreased, but the differences between the two groups were smaller (Fig. 2c).

Considering very consistent grouping of the genotypes and a low number of repetitions in measurements for individual genotypes, to ensure the significant differences in statistical analyses, in the rest of the manuscript, we will compare the two groups (HEX vs. TET) instead of individual genotypes.

In addition to C and R1, Fig. 2 shows the results of R2 variant, i.e., the photosynthetic rate, V_{Cmax} and J_{max} after 3–5 days of recovery. While the HEX group did not recover at all, the recovery in the TET group was significant. In this group, the J_{max}-to-V_{cmax} ratio was not affected by the period of heat stress, while in the HEX group, we observed a decrease in J_{max}/V_{cmax}, with no recovery between R1 and R2, indicating that in the HEX group, the heat stress episode caused an imbalance between the electron transport-related

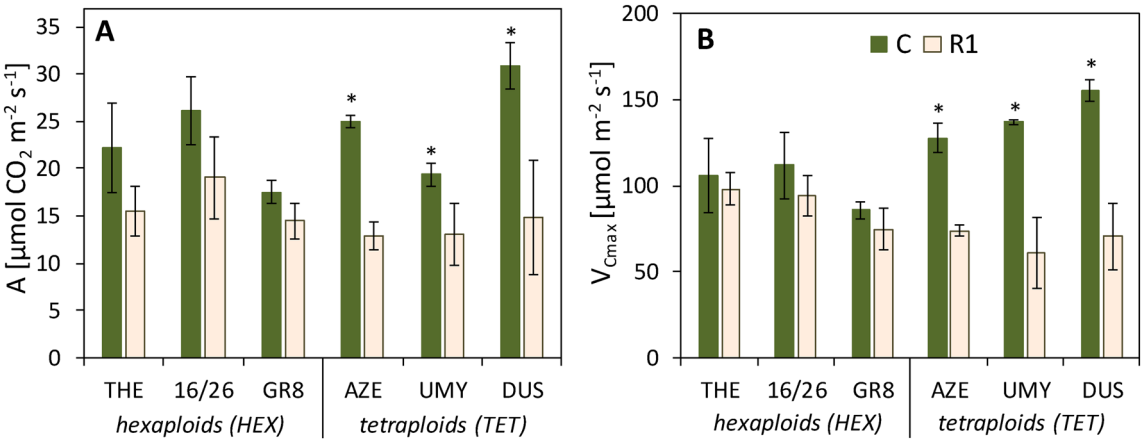

Fig. 1 **a** Net photosynthesis rate (*A*), and **b** the maximum carboxylation rate (V_{Cmax}) in hexaploid wheat breeds (THE—Thesee; 16/26—SLO-16/26; GR8—GRC-867) and in tetraploid wheat breeds (AZE—AZESVK2009-97, UMY—Unmedpur M., DUS—Dušan) in control plants (**c**) and plants exposed to heat stress, measured at the beginning of the post-heat stress recovery phase (R1). The mean values ± standard error ($n = 3$) are presented. Asterisks (*) indicate the significant difference of values observed in the R1 variant at $P < 0.05$ level by Duncan test when compared to the control in individual genotypes

processes and the carboxylation processes, although the TET group remained balanced.

PSII and PSI photochemistry in recovery after prolonged heat stress

The prolonged heat stress had a moderate but statistically significant effect on PSII photochemistry, with a decrease in F_v/F_m by 0.06 in HEX and 0.09 in TET in R1. Similar to the gas exchange response, the subsequent recovery in R2 was efficient in TET, while in HEX, F_v/F_m had not recovered. However, all the observed decreases in the maximum quantum efficiency of PSII were relatively low, indicating rather low irreversible damage of PSII units (Fig. 3a).

The decrease in P_m was much more evident (Fig. 3d), indicating a significant decrease in the total pool of PSI reaction centers (RCs) that can be oxidized, i.e., the active PSI RCs. In R1, the heat stress led to a decrease in P_m by ~ 30% in HEX, and the decrease was almost 50% in TET. In the next stage (R2), a moderate recovery was observed in both groups, but the pool of active PSI RCs was still lower by 21% in HEX and 37% in TET than in the control plants. The PSII and PSI quantum yields measured under actinic illumination followed the trends observed in CO_2 assimilation, with a greater decrease in the values in TET than HEX in R1, but with a better recovery of TET than HEX in R2 (Fig. 3b,e). The quantum yield of PSI, *Y*(I), was lowered more than the PSII quantum yield, *Y*(II). The PSI quantum yield represents the fraction of active PSI at a given light intensity engaged both in linear and cyclic electron flow, whereas the PSII quantum yield only indicates linear flow, and a stronger decrease in *Y*(I) indicates a decrease in cyclic electron flow. A similar trend was observed also for the parameter indicating the nonphotochemical quenching (NPQ), but the level of recovery in R2 was higher than that for the other parameters measured (Fig. 3c). The parameter *Y*(NA) representing the quantum yield of nonphotochemical quenching induced by the limitation at the PSI acceptor side showed an inverse trend compared to most of the previously assessed parameters, with a maximum in R1 and a decrease in R2 back to the initial level in TET, whereas the values in HEX were still higher than those in the control (Fig. 3f). As this parameter represents the redox poise (negative charge) of the PSI electron acceptors, we can state that overreduction of the PSI acceptor side occurred in both groups in R1 (being more severe in TET), but the overreaction persisted only in the HEX group in R2.

The proton transport responses after impact of prolonged heat stress

The proton transport on the transthylakoid membrane was estimated by noninvasive ECS measurement. By analysis of the ECS decay, we determined the magnitude of proton conductivity, g_H^+, and the amplitude of the ECS signal (ESC_t) as a rough estimate of the proton motive force, *pmf*, and its two components, ΔpH and Δψ. In the R1 phase, the g_H^+ was lower on average by 22%, with no significant difference between the HEX and TET groups. In the R2 phase, when heat-affected plants were returned to normal conditions and measured after 3–5 days, the g_H^+ increased to 89% of the control value on average (Fig. 4a). The ECS_t was higher by 48% than in the control on average in the R1 phase, and in the R2 phase, the TET group responded by a decrease of 45%, while that of the HEX group decreased by only 11% (Fig. 4b). In response to prolonged heat, the proton gradient,

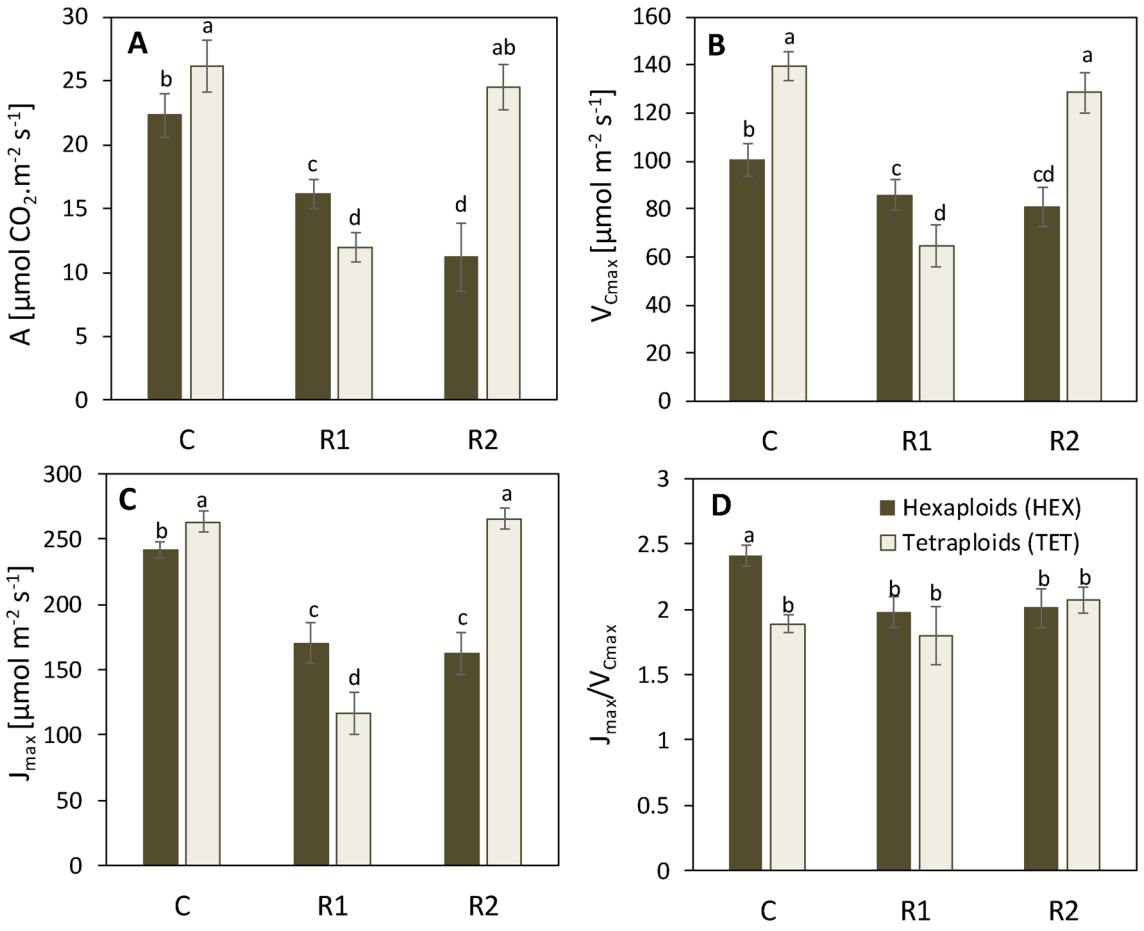

Fig. 2 Results of gas exchange analyses and subsequent analyses of A/C_i curves measured in two groups of genotypes: HEX—hexaploid, and TET—tetraploid bread wheat genotypes. **a** The net photosynthesis rate (*A*), **b** the maximum carboxylation rate (V_{Cmax}), **c** the maximum electron transport rate (J_{max}), and **d** their ratio (J_{max}/V_{Cmax}) in control plants (*C*) and plants exposed to heat stress, measured at the beginning of the post-heat stress recovery phase (R1) and after 3–5 days of recovery at moderate temperature level (R2). The mean values ± standard errors from 6–9 measurements are presented. Different small letters (a, b, c) indicate the significant difference of values at the $P < 0.05$ level, based on the Duncan test

ΔpH, decreased to almost one-third of the control value on average, but in response to the recovery phase, the value in the TET group increased to a value equal to twofold that in HEX plants (Fig. 4c). The electric component of *pmf*, Δψ, however, increased to almost threefold on average in response to prolonged heat (R1), but interestingly, the value in the recovery phase (R2) decreased only by 31% in the HEX group, whereas it recovered by 87% in the TET group (Fig. 4d).

Correlation analyses

To better understand the relationships between the processes related to the proton transport and the main photosynthetic characteristics related both to CO_2 assimilation and photoprotective responses in recovery from the heat stress, we analyzed the correlations between the parameters derived from the DIRK analysis of ECS and the other main characteristics assessed in this study (Fig. 5). The amplitude of the ECS signal (Fig. 5a–d) correlated negatively with the CO_2 assimilation, PSII electron transport rate and NPQ, while the correlation with the acceptor side limitation of PSI was positive. Analysis of the two components of the ECS signal (Fig. 5e–l), namely the osmotic component of *pmf* – ΔpH and electric component of *pmf* – Δψ, indicated that the trend of ECS_t was mainly influenced by Δψ values, the increase in which was higher than the lower decrease in ΔpH under heat stress conditions.

As expected, the transthylakoid proton gradient (ΔpH) showed a clear positive correlation with NPQ, and a positive correlation was also observed in the relationships between the ΔpH and CO_2 assimilation rate (A) and the rate of linear electron transport (ETR_{PSII}). However, there was a negative correlation between ΔpH and the reduction

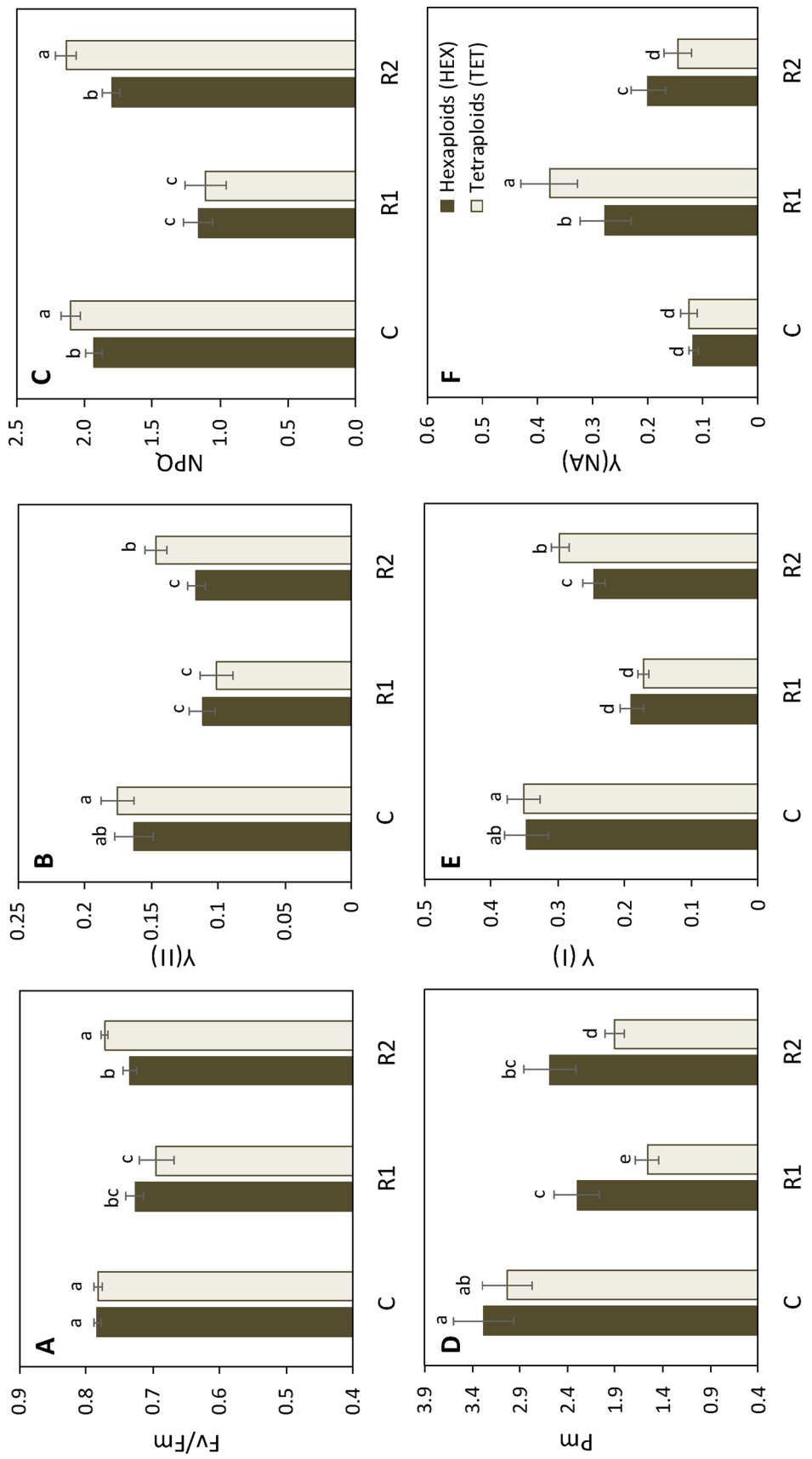

Fig. 3 Results of simultaneous PSII/PSI analyses under actinic light illumination, measured in two groups of genotypes: HEX—hexaploid, and TET—tetraploid bread wheat genotypes. **a** Maximum quantum yield of PSII photochemistry—F_v/F_m, **b** PSII quantum yield—Y(II), **c** Nonphotochemical quenching ratio (NPQ), **d** Maximum amplitude of the P700 signal, providing an estimate of active PSI units—P_m, **e** PSI quantum yield—Y(I), and **f** Quantum yield of nonphotochemical energy dissipation of reaction centers due to PSI acceptor side limitation, recorded in control plants (*C*) and plants exposed to heat stress, measured at the beginning of the post-heat stress recovery phase (R1) and after 3–5 days of recovery at moderate temperature level (R2). The mean values ± standard error from 6 to 9 measurements are presented. Different small letters (a, b, c, d) indicate the significant difference of values at the $P<0.05$ level, based on the Duncan test

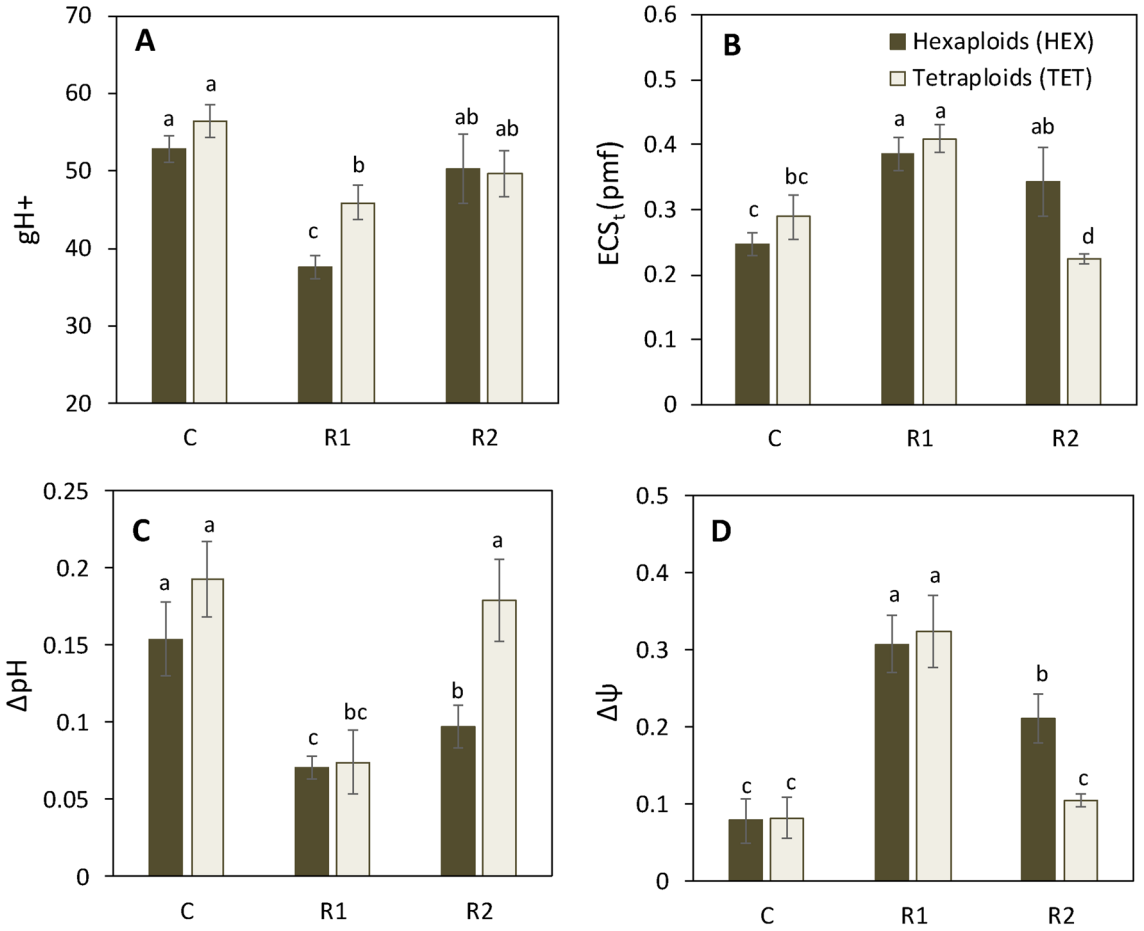

Fig. 4 Results of DIRK analysis of the ECS signal recorded after the actinic light illumination was switched off. The values were measured in two groups of genotypes: HEX—hexaploid, and TET—tetraploid bread wheat genotypes. **a** Proton conductivity – g_H^+, **b** Maximum amplitude of ECS signal providing an estimate of the proton motive force (*pmf*)—ECS_t, **c** Transthylakoid proton gradient—ΔpH, and **d** Electric membrane potential—Δψ, recorded in control plants (*C*) and plants exposed to heat stress, measured at the beginning of the post-heat stress recovery phase (R1) and after 3–5 days of recovery at moderate temperature level (R2). The mean values ± standard error from 6 to 9 measurements are presented. Different small letters indicate the significant difference of values at $P < 0.05$ (Duncan test)

of the PSI acceptor side (parameter Y(NA)). Inverse trends were recorded for the parameter Δψ. The correlations observed for the proton conductance (g_H^+) followed the trends observed in the case of ΔpH, but the correlations were mostly weak (Fig. 5m–p).

Discussion

Heat stress effects on photosynthesis have been extensively studied for numerous crops and genotypes. It is widely accepted that the enzymes of the Calvin–Benson cycle are prone to heat stress. Moderate thermal stress represents a hindrance for the carbon assimilation system, which is sensitive to high temperatures and can be easily inhibited (Feller et al. 1998; Berry and Bjorkman 1980; Weis 1981; Sharkey 2005). Under such conditions, the Rubisco activity decreases along with the rate of photosynthesis (Law and Crafts-Brandner 1999), though the enzyme itself is not heat labile. The Rubisco activase is the high-temperature-sensitive component in the carbon assimilation system (Salvucci and Crafts-Brandner 2004; Sharkey 2005). The decrease in enzyme activity responds to actual temperature levels and recovers briefly under the optimum temperature level. However, the heat stress may be associated with the decrease in photosynthetic capacity, with a slow and often incomplete recovery of photosynthetic capacity. A proteomic study of Das et al. (2016) has shown that crucial proteins such as ATP synthase, HCF136 (PSII stability factor) and oxygen-evolving enhancer protein 2–1 in PSII as well as FNR at PSI are heat sensitive, providing one possible explanation for the prolonged heat stress effects. Our previous studies (Brestic et al. 2016; Chovancek et al. 2019) indicated that high-temperature conditions in wheat were associated

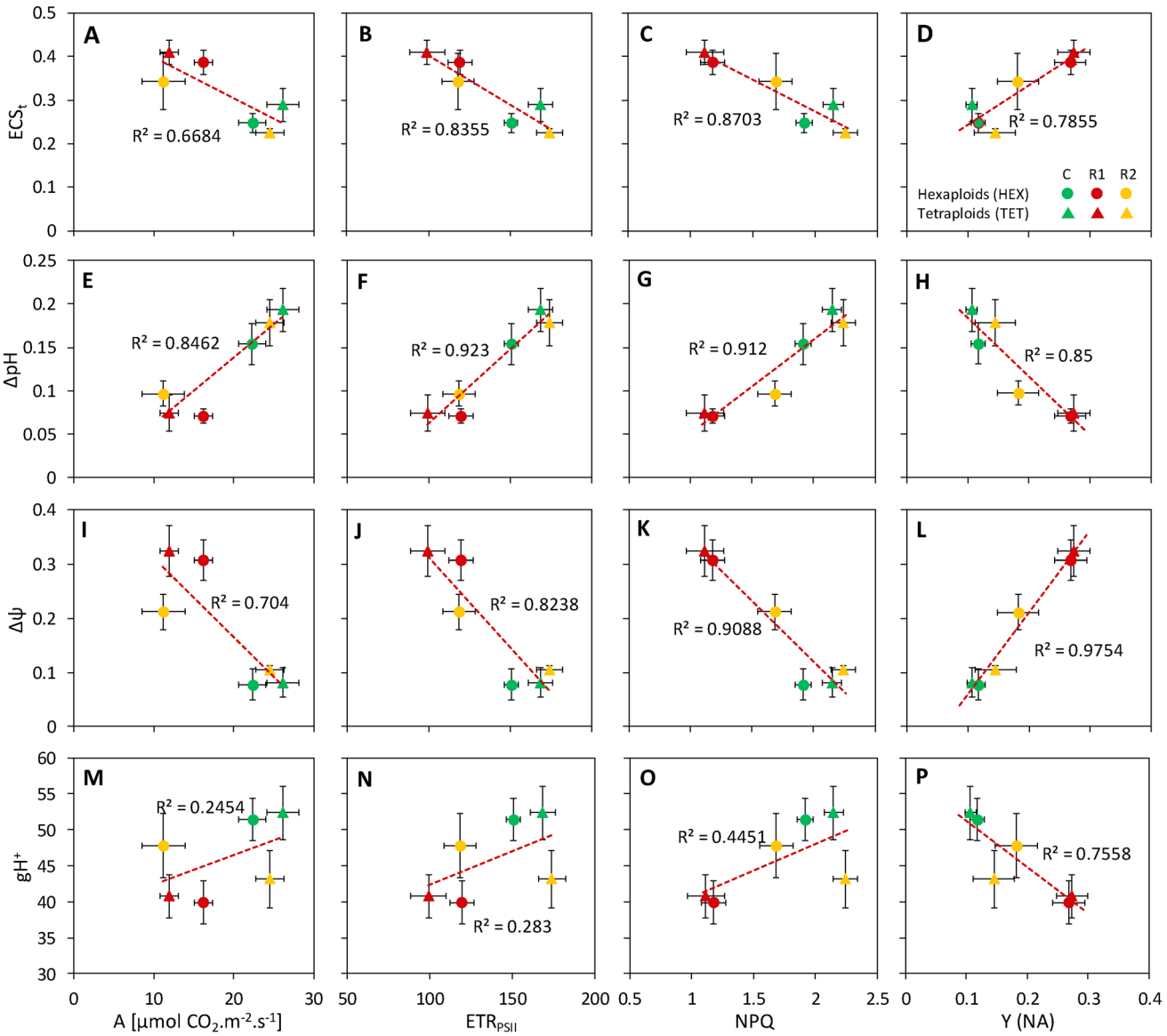

Fig. 5 Correlations between the parameters derived from simultaneous analysis of the gas exchange and chlorophyll fluorescence (A and ETR_{PSII}) or dual PSII/PSI records (NPQ, Y(NA)) and the parameters derived from the DIRK analysis of ECS kinetics (ECSt, ΔpH, Δψ and gH^+). The points represent the mean values ± SE. The dashed lines represent the fitted linear regression estimates, with the determination coefficient (R^2) for each correlation. The different colors of the points represent the variants (*C*, R1 and R2), and the different shape of the points indicates two groups differing in responses (circles—hexaploids (HEXs), triangles—tetraploids (TETs)); see the legend in the upper right panel

with inefficient regulation of electron transport during the stress but also after the stress relief, generating conditions for excessive ROS formation due to overreduction of the PSI acceptor side. The redox state and quantity of PSI is crucial for survival of C3 plants under adverse conditions, as oxidation of PSI leads to suppression of ROS production at PSI (Shimakawa and Miyake 2018, 2019; Miyake 2020). Thus, in addition to direct heat effects, the oxidative damage of key photosynthetic complexes may play a major role in the post-heat stress period, influencing both the photosynthetic capacity and recovery process after heat stress relief, which were previously shown to be sensitive to reductions in capacity for photosynthetic electron transport and photoprotection in heat-stressed leaves in the field (Schrader et al. 2007; Wise et al. 2004).

The photoprotection and protection against oxidative damage in the chloroplast is a result of the proper interplay of various processes and redox signaling systems, with the central position of the proton transport and its regulation (Zhang and Sharkey 2009). The proton transport is related to

the activity of the chloroplast ATP synthase, which responds to the demand created by photosynthesis during steady-state metabolism. Changing levels of CO_2 induce different proton conductivities of ATP synthase, g_H^+ (Avenson et al. 2004). The chloroplast ATP synthase is driven by the proton motive force, *pmf*, which consists of the proton gradient, ΔpH, and electric membrane potential, Δψ (Cruz et al. 2001). The regulation of *pmf* must satisfy two conflicting physiological demands: (i) producing enough ATP for carbon assimilation processes and (ii) avoiding damage by ROS produced in high-light and/or adverse conditions. The *pmf* is shown to be an optimal key regulator of this tradeoff (Huang et al. 2018). Electrochromic bandshift (ECS) measurements represent a unique noninvasive tool that offers insight into proton transport-related processes, providing estimates of g_H^+, *pmf*, Δψ and ΔpH (Witt 1971; Joliot and Joliot 1989; Klughammer et al. 2013; Bailleul et al. 2010). In our experiment, the analyses of ECS decay after light switch-off, following a longer exposure of leaves to a high actinic light, indicated an increase in ECS_t (representing an estimate of *pmf*) in heat-stressed plants after a short-time recovery compared to stress and, in general, an inverse relationship between the photosynthetic rate and the ECS_t amplitude (Fig. 5a). An increase in ECS_t under stress conditions is usually attributed to an increase in the transthylakoid proton gradient due to accumulation of H^+ in the thylakoid lumen as a result of lower demand for ATP synthesis when the carbon assimilation is reduced.

The acidification of thylakoid lumen leads to downregulation of electron transport and upregulation of the thermal dissipation of absorbed light energy by the photosystem II, which can well be indicated by high values of the NPQ parameter derived from PAM fluorescence measurements (Ruban 2016). However, in our experiments, we found a negative correlation between the ECS_t and NPQ values (Fig. 5c). The subsequent analysis of the ECS decay kinetics (Avenson et al. 2004) confirmed that the increase in ECS_t in plants previously exposed to heat stress was not connected with a high ΔpH value, but rather reflects an increase in the electric membrane potential, Δψ. However, the correlations between ΔpH and NPQ were clear and positive (Fig. 5g), confirming that the low ΔpH in stressed plants is not an artifact but corresponds to the redox state of the thylakoid membranes in the chloroplast.

However, a high Δψ was clearly associated with the state in which photosynthesis was low (Fig. 5i), but the expected photoprotective responses were not efficient enough, considering low NPQ values, and especially, high Y(NA), indicating insufficient downregulation of linear electron transport connected with a strong reducing burst at the acceptor side of PSI (Yamori et al. 2016). The related photoinhibitory damage was observed both on the PSII level (decrease in F_v/F_m; Fig. 3a) as well as the PSI level (decrease in P_m; Fig. 3d). In the TET group, in which the Δψ was lowered to the initial value in a longer recovery period (R2), F_v/F_m was fully recovered. However, in the HEX group, the Δψ was significantly higher than that of the control, and F_v/F_m remained low. This result is consistent with previous evidence that a high Δψ state induces oxidative photodamage of the thylakoid components under fluctuating light (Davis et al. 2016), as Δψ will cause a rise in energy levels of particular components of the electron transport chain connected with formation of reactive oxygen species (Vos et al. 1991; Johnson et al. 1995). Although there are several processes that may contribute to an increase in the Δψ component of the *pmf*, a high correlation between Δψ and Y(NA) suggests that the overreduction of the electron transport chain, especially at the PSI acceptor side, may represent an important source of the negative charge at the stromal side of the thylakoid membrane.

Another interesting finding was the clear correlation between the CO_2 assimilation, linear electron transport rate, V_{Cmax} or J_{max} (not shown, but clear from a comparison of the trends in Fig. 2 and Fig. 4) and Δψ and ΔpH values (Fig. 5). Our previous results in experiments with wheat have shown that a decrease in CO_2 assimilation (e.g., due to stomata closure) leads to an increase in ΔpH and not so much in Δψ (Zivcak et al. 2014), which is consistent with the recent mechanistic understanding of this proton transport and its regulation (Walker et al. 2020; Kramer et al. 2004). Hence, the limitation at the acceptor side of the linear electron transport cannot be responsible for observed trends, i.e., decrease in ΔpH and increase in Δψ values. However, there is a question of whether the redox state of the electron transport chain could be responsible for the downregulation of the carbon assimilation processes. As we did not observe the same trend of the J_{max}/V_{Cmax} ratio and the CO_2 assimilation rate (Fig. 2), we have no direct argument supporting the hypothesis that the linear electron transport was the major factor directly limiting CO_2 assimilation. However, we cannot fully exclude that model underestimated the V_{Cmax} values, and the real value could be higher, but rates were constrained by the electron transport (J_{max}) at all CO_2 concentrations. Moreover, there is still a possibility that the activity of the enzymes was influenced by the redox state of the electron transport chain via redox signaling pathways. There is clear evidence that the Calvin cycle enzymes can be activated/inactivated according to the states of both by the NADPH/$NADP^+$ ratio and/or ATP/ADP ratio (Dietz and Pfannschmidt 2011), but regulation of the activity of photosynthetic enzymes via the thioredoxin/ferredoxin system located at the acceptor side of photosystem I may also play an important role in enzyme activation (Meyer et al. 2012; Schürmann and Buchanan 2008; Lemaire et al. 2007; Wolosiuk and Buchanan 1977). The hypothesis on the link between the enzyme activity and the redox state of the photosystem I acceptor side is strongly

supported by the results of our previous experiment (Zivcak et al. 2015), in which a short sequence of saturation pulses led to inactivation of a significant number of PSI reaction centers, leading to a similar state of electron and proton transport as that observed after the heat stress period (low P_m, NPQ, ΔpH; high Y(NA) and Δψ values), associated with a dramatic decrease in the photosynthetic capacity persisting for several days. Our analyses clearly indicated that the limited electron transport capacity cannot be responsible for a high decrease in photosynthesis under high-light conditions, providing strong arguments in favor of redox regulation issues. Unlike the previous experiments, recent experiments clearly showed that a low number of active PSI reaction centers indicated by parameter P_m (Fig. 3d) was not associated with a lower photosynthetic rate (in R2, P_m in TET was lower than that in HEX, but the net photosynthesis was higher), indicating that the values of ΔpH, Δψ and Y(NA), rather than the level of PSI inactivation per se, determine the photoprotection and photosynthetic capacity. As buildup of the transthylakoid proton gradient will eliminate the excessive values of Δψ and *Y*(NA), the capacity to maintain or recover a high value of ΔpH under high-light conditions after heat stress appears to be crucial for full recovery of photosynthesis in the post-heat stress period.

An additional question is what mechanism can be responsible for the differences in Δψ and ΔpH between the two groups of genotypes. The ΔpH is increased by production of H^+ at OECs and with the help of reduced PQs, while it is depleted by the activity of ATP synthases. Indeed, the OEC of PSII appears to be highly sensitive to high-temperature stress, as exemplified by various studies (Katoh and San Pietro 1967; Berry and Bjorkman 1980; Mamedov et al. 1993; Havaux and Tardy 1996). However, the level of PSII damage observed in our study was not high enough to explain a low ΔpH. An alternative explanation was provided by Zhang and Sharkey (2009), who argued that the leakiness of the thylakoid membrane for H^+ may contribute to an increased g_H^+ in the light and thus a low ΔpH. Normally, the proton conductivity values estimated from the ECS decay (g_H^+) broadly reflect the activity of ATP synthase; i.e., g_H^+ represents the effective conductivity of the CFO-CF1 ATP synthase to protons (Takizawa et al. 2007b; Kohzuma et al. 2009). However, it was shown that after heat stress, the proton conductivity greatly increases, which is clearly associated with the leaks of H^+ through the thylakoid membrane (Havaux et al. 1996). Although based on the values of g_H^+ only, we were not able to recognize the presence or absence of the proton leaks (Fig. 4). We found some effects that indirectly confirm H^+ leakage across the thylakoid membranes. The steady-state proton flux estimated from ECS_t multiplied by g_H^+ is normally positively correlated with the linear electron transport rate (Kohzuma et al. 2009), and hence, the values of proton flux to the electron transport ratio were formerly in a relatively narrow range. However, this outcome was not the case in our experiment (Fig. 6), in which the proton flux values in poorly recovered samples were much higher than expected according to the ETR_{PSII} values (Fig. 6a), and the proton flux per linear electron transport unit (ν_{H+}/ETR_{PSII}) varied widely, reaching even threefold higher values in poorly recovered samples than the control. The proton flux estimated from the analysis of the DIRK kinetics of the ECS signal was not proportional to the linear electron transport, which can be well explained by proton leakage. In a specific cases when plants have been exposed to heat, the g_H^+ values estimated from the exponential decay of the ECS signal do not represent the real activity of the ATP synthase only, but

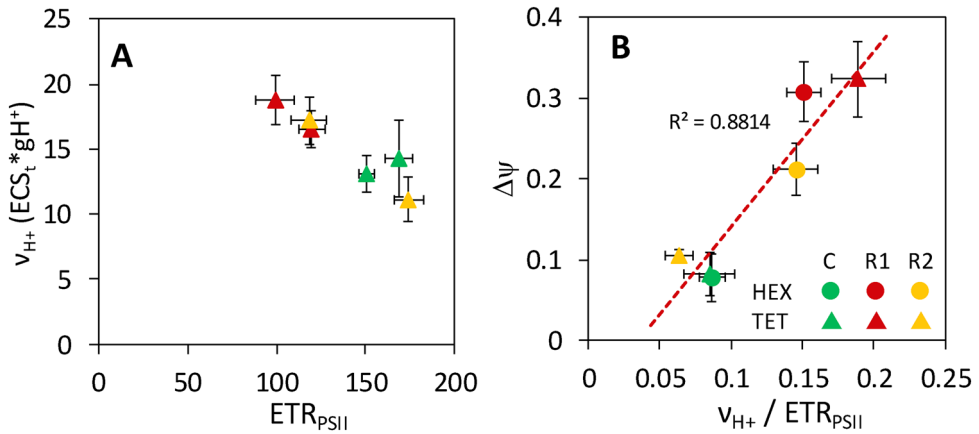

Fig. 6 **a** Measurements of the linear electron transport rate (ETR_{PSII}) and estimates of the proton flux ($\nu_{H+} = ECS_t{*}g_H^+$) per variant. **b** The correlation between the proton flux per linear electron transport unit and Δψ component of the *pmf*. The points represent the mean values ± SE. The dashed lines represent the fitted linear regression estimates with the determination coefficient (R^2) for each correlation. The different colors of the points represent the variants (*C*, R1 and R2) and the different shape of the points indicates two groups (circles—hexaploids (HEX), triangles—tetraploids (TET)); see the legend

also the leaks decreasing the efficiency of converting the proton motive force into ATP.

Excessively fast proton efflux (via ATP synthase and leaks) cannot be efficiently supplied by the proton influx generated by the activity of the linear electron flow, resulting in a low ΔpH and a high Δψ, which is documented by a correlation between the proton flux per linear transport unit and Δψ (Fig. 6b). In this respect, the ability to recover full integrity of thylakoid membrane together with the processes supporting the redox balance appears to be crucial for efficient recovery of photosynthetic functions. The contribution of alternative electron pathways (Tan et al. 2020), cyclic electron flow (Wang et al. 2015) or regulation of ATP synthase activity (Huang et al. 2018) can play significant roles in maintaining the balance of photochemical processes, especially the ATP/NADPH ratio, which can be crucial for proper functioning of photosynthetic metabolism and support of recovery processes (Shikanai et al. 2002). However, the specific molecular mechanisms responsible for the differences in recovery of photosynthesis in the two groups of wheat genotypes need to be further examined.

One of the important findings of this study is that the two different-ploidy genotype groups show different responses to prolonged heat stress. Though the hexaploid bread wheat species (*T. aestivum* L.) appear to be less prone to heat stress than the tetraploid species (*T. durum* Desf., *T. turgidum* L., *T. timopheevi* Zhuk.), in terms of the ability to recover from heat stress, the tetraploids were superior. It is important to emphasize that these two groups are genetically quite distant, as all the tetraploids have the same genomes ($2n = 4x = 28$, AABB), whereas the hexaploid bread wheat ($2n = 6x = 42$, AABBDD) contains an additional D-genome originating from the wild relative *Aegilops tauschii* ($2n = 2x = 14$, DD). Hybridization of this wild species with cultivated tetraploid emmer wheat *T. turgidum* produced *T.* aestivum, which has been cultivated and bred for more than eight thousand years (Wang et al. 2013).

The genetic differences between the tetraploid and hexaploid species were previously found to also be associated with the differences in photosynthetic responses. For example, the D-genome in hexaploid wheat was found to be responsible for differences in the flag leaf area, gas exchange, chlorophyll content, and net photosynthesis rate (Olsen et al. 2015; Blanco et al. 2000). The tests of synthetic polyploids demonstrated that addition of the D-genome into synthesized hexaploid wheat species led to a decrease in the photosynthetic rate, although the depression of photosynthesis was dependent on the source of the D-genome (Watanabe et al. 1997). Moreover, a recent study has shown that different-ploidy levels may play an important regulatory role in photochemistry and antioxidative systems of plants (Mao et al. 2018), which fairly corresponds to the findings presented in this study. In that way, our results contribute to the topic of the interaction between the wheat ploidy level and the photosynthetic responses by the evidence on the ploidy-related variations in response to high temperature and recovery, associated with the differences in regulation of electron and proton transport.

Conclusions

Based on the results of these experiments, we identified that the two different-ploidy groups of wheat genotypes clearly differ in their responses to heat stress. The analyses of gas exchange, simultaneous measurements of PSI and PSII photochemistry and measurements of electrochromic bandshift (ECS) have consistently shown that the photosynthetic and photoprotective function in leaves of tetraploids was almost fully recovered after several days, while that of hexaploids was still rather low. A poor recovery was associated with an overly reduced acceptor side of photosystem I, as well as high values of the electric membrane potential (Δψ component of the proton motive force, *pmf*) in the chloroplast. Our results suggest that a high Δψ can be associated with an excessive proton flux via the thylakoid membrane due to membrane leakiness that prevents the accumulation of H^+ in the thylakoid lumen. However, a good recovery of photosynthetic capacity and photoprotective functions was clearly associated with an enhanced proton gradient (ΔpH component of the *pmf*), thus demonstrating a key role of efficient regulation of proton transport to ensure buildup of the transthylakoid proton gradient needed for photosynthesis restoration after high-temperature episodes.

Acknowledgments This work was supported by the Ministry of Education, Science, Research and Sport of the Slovak Republic under the projects VEGA-1-0589-19 and VEGA 1-0683-20 and the Slovak Research and Development Agency project APVV-18-465. This work was also supported by the project OPVaI-VA/DP/2018/No. 313011T813. SIA was supported by the foundation of "systems of natural and artificial photosynthesis" (FEES-2021-0012).

Compliance with ethical standards

Conflict of interest The authors declare that they have no conflicts of interest.

References

Allakhverdiev SI, Kreslavski VD, Klimov VV, Los DA, Carpentier R, Mohanty P (2008) Heat stress: an overview of molecular responses in photosynthesis. Photosynth Res 98(1–3):541–550. https://doi.org/10.1007/s11120-008-9331-0

Almeselmani M, Deshmukh PS, Sairam RK, Kushwaha SR, Singh TP (2006) Protective role of antioxidant enzymes under high temperature stress. Plant Sci 171(3):382–388. https://doi.org/10.1016/j.plantsci.2006.04.009

Armbruster U, Carrillo LR, Venema K, Pavlovic L, Schmidtmann E, Kornfeld A, Jahns P, Berry JA, Kramer DM, Jonikas MC (2014) Ion antiport accelerates photosynthetic acclimation in fluctuating light environments. Nat Commun 5:5439. https://doi.org/10.1038/ncomms6439

Avenson TJ, Cruz JA, Kramer DM (2004) Modulation of energy-dependent quenching of excitons in antennae of higher plants. Proc Natl Acad Sci U S A 101(15):5530–5535. https://doi.org/10.1073/pnas.0401269101

Avenson TJ, Cruz JA, Kanazawa A, Kramer DM (2005) Regulating the proton budget of higher plant photosynthesis. Proc Natl Acad Sci U S A 102(27):9709–9713. https://doi.org/10.1073/pnas.0503952102

Bailleul B, Cardol P, Breyton C, Finazzi G (2010) Electrochromism: a useful probe to study algal photosynthesis. Photosynth Res 106(1–2):179

Baker NR (2008) Chlorophyll fluorescence: a probe of photosynthesis in vivo. Annu Rev Plant Biol 59(1):89–113. https://doi.org/10.1146/annurev.arplant.59.032607.092759

Baker NR, Harbinson J, Kramer DM (2007) Determining the limitations and regulation of photosynthetic energy transduction in leaves. Plant, Cell Environ 30(9):1107–1125. https://doi.org/10.1111/j.1365-3040.2007.01680.x

Berry J, Bjorkman O (1980) Photosynthetic response and adaptation to temperature in higher plants. Annu Rev Plant Physiol 31(1):491–543

Blanco IA, Rajaram S, Kronstad WE, Reynolds MP (2000) Physiological performance of synthetic hexaploid wheat-derived populations. Crop Sci 40(5):1257–1263. https://doi.org/10.2135/cropsci2000.4051257x

Brestic M, Zivcak M, Kalaji HM, Carpentier R, Allakhverdiev SI (2012) Photosystem II thermostability in situ: Environmentally induced acclimation and genotype-specific reactions in *Triticum aestivum* L. Plant Physiol Biochem 57:93–105. https://doi.org/10.1016/j.plaphy.2012.05.012

Brestic M, Zivcak M, Kunderlikova K, Allakhverdiev SI (2016) High temperature specifically affects the photoprotective responses of chlorophyll b-deficient wheat mutant lines. Photosynth Res 130(1–3):251–266. https://doi.org/10.1007/s11120-016-0249-7

Brestic M, Zivcak M, Hauptvogel P, Misheva S, Kocheva K, Yang X, Li X, Allakhverdiev SI (2018) Wheat plant selection for high yields entailed improvement of leaf anatomical and biochemical traits including tolerance to non-optimal temperature conditions. Photosynth Res 136(2):245–255. https://doi.org/10.1007/s11120-018-0486-z

Carraretto L, Formentin E, Teardo E, Checchetto V, Tomizioli M, Morosinotto T, Giacometti GM, Finazzi G, Szabo I (2013) A thylakoid-located two-pore K+ channel controls photosynthetic light utilization in plants. Science 342(6154):114–118. https://doi.org/10.1126/science.1242113

Chovancek E, Zivcak M, Botyanszka L, Hauptvogel P, Yang X, Misheva S, Hussain S, Brestic M (2019) Transient heat waves may affect the photosynthetic capacity of susceptible wheat genotypes due to insufficient photosystem I photoprotection. Plants (Basel). https://doi.org/10.3390/plants8080282

Cruz JA, Sacksteder CA, Kanazawa A, Kramer DM (2001) Contribution of electric field (Delta psi) to steady-state transthylakoid proton motive force (pmf) in vitro and in vivo control of pmf parsing into Delta psi and Delta pH by ionic strength. Biochemistry 40(5):1226–1237. https://doi.org/10.1021/bi0018741

Cruz JA, Avenson TJ, Kanazawa A, Takizawa K, Edwards GE, Kramer DM (2005) Plasticity in light reactions of photosynthesis for energy production and photoprotection. J Exp Bot 56(411):395–406. https://doi.org/10.1093/jxb/eri022

Das A, Eldakak M, Paudel B, Kim DW, Hemmati H, Basu C, Rohila JS (2016) Leaf proteome analysis reveals prospective drought and heat stress response mechanisms in soybean. Biomed Res Int 2016:6021047. https://doi.org/10.1155/2016/6021047

Davis GA, Kanazawa A, Schottler MA, Kohzuma K, Froehlich JE, Rutherford AW, Satoh-Cruz M, Minhas D, Tietz S, Dhingra A, Kramer DM (2016) Limitations to photosynthesis by proton motive force-induced photosystem II photodamage. Elife. https://doi.org/10.7554/eLife.16921

Davis GA, Rutherford AW, Kramer DM (2017) Hacking the thylakoid proton motive force for improved photosynthesis: modulating ion flux rates that control proton motive force partitioning into Deltapsi and DeltapH. Philos Trans R Soc Lond B Biol Sci 372(1730). https://doi.org/10.1098/rstb.2016.0381

Dietz K-J, Pfannschmidt T (2011) Novel regulators in photosynthetic redox control of plant metabolism and gene expression. Plant Physiol 155(4):1477–1485. https://doi.org/10.1104/pp.110.170043

Driedonks N, Rieu I, Vriezen WH (2016) Breeding for plant heat tolerance at vegetative and reproductive stages. Plant Reprod 29(1–2):67–79. https://doi.org/10.1007/s00497-016-0275-9

Duan Z, Kong F, Zhang L, Li W, Zhang J, Peng L (2016) A bestrophin-like protein modulates the proton motive force across the thylakoid membrane in Arabidopsis. J Integr Plant Biol 58(10):848–858. https://doi.org/10.1111/jipb.12475

Ethier GJ, Livingston NJ (2004) On the need to incorporate sensitivity to CO_2 transfer conductance into the Farquhar–von Caemmerer-Berry leaf photosynthesis model. Plant Cell Environ 27:137–153. https://doi.org/10.1111/j.1365-3040.2004.01140.x

Farquhar GD, von Caemmerer S, Berry JA (1980) A biochemical model of photosynthetic CO_2 assimilation in leaves of C 3 species. Planta 149(1):78–90. https://doi.org/10.1007/BF00386231

Feller U, Crafts-Brandner SJ, Salvucci ME (1998) Moderately high temperatures inhibit ribulose-1,5-bisphosphate carboxylase/oxygenase (rubisco) activase-mediated activation of rubisco. Plant Physiol 116(2):539–546. https://doi.org/10.1104/pp.116.2.539

Hasanuzzaman M, Nahar K, Alam MM, Roychowdhury R, Fujita M (2013) Physiological, biochemical, and molecular mechanisms of heat stress tolerance in plants. Int J Mol Sci 14(5):9643–9684. https://doi.org/10.3390/ijms14059643

Havaux M, Tardy F (1996) Temperature-dependent adjustment of the thermal stability of photosystem II in vivo: possible involvement of xanthophyll-cycle pigments. Planta 198(3):324–333

Havaux M, Tardy F, Ravenel J, Chanu D, Parot P (1996) Thylakoid membrane stability to heat stress studied by flash spectroscopic measurements of the electrochromic shift in intact potato leaves: influence of the xanthophyll content. Plant, Cell Environ 19(12):1359–1368. https://doi.org/10.1111/j.1365-3040.1996.tb00014.x

Hede A, Skovmand B, Reynolds M, Crossa J, Vilhelmsen A, Stølen O (1999) Evaluating genetic diversity for heat tolerance traits in Mexican wheat landraces. Genet Resour Crop Evol 46(1):37–45

Herdean A, Nziengui H, Zsiros O, Solymosi K, Garab G, Lundin B, Spetea C (2016a) The Arabidopsis thylakoid chloride channel AtCLCe functions in chloride homeostasis and regulation of photosynthetic electron transport. Front Plant Sci 7:115. https://doi.org/10.3389/fpls.2016.00115

Herdean A, Teardo E, Nilsson AK, Pfeil BE, Johansson ON, Unnep R, Nagy G, Zsiros O, Dana S, Solymosi K, Garab G, Szabo I, Spetea C, Lundin B (2016b) A voltage-dependent chloride channel fine-tunes photosynthesis in plants. Nat Commun 7:11654. https://doi.org/10.1038/ncomms11654

Huang W, Tikkanen M, Cai YF, Wang JH, Zhang SB (2018) Chloroplastic ATP synthase optimizes the trade-off between photosynthetic CO_2 assimilation and photoprotection during leaf maturation. Biochim Biophys Acta Bioenerg. https://doi.org/10.1016/j.bbabio.2018.06.009

Johnson GN, Rutherford AW, Krieger A (1995) A change in the midpoint potential of the quinone QA in photosystem II associated with photoactivation of oxygen evolution. Biochim Biophys Acta 1229(2):202–207

Joliot P, Joliot A (1989) Characterization of linear and quadratic electrochromic probes in *Chlorella sorokiniana* and *Chlamydomonas reinhardtii*. Biochim Biophys Acta 975(3):355–360

Kanazawa A, Ostendorf E, Kohzuma K, Hoh D, Strand DD, Sato-Cruz M, Savage L, Cruz JA, Fisher N, Froehlich JE, Kramer DM (2017) Chloroplast ATP synthase modulation of the thylakoid proton motive force: implications for photosystem I and photosystem II photoprotection. Front Plant Sci 8:719. https://doi.org/10.3389/fpls.2017.00719

Katoh S, San Pietro A (1967) Ascorbate-supported NADP photoreduction by heated Euglena chloroplasts. Arch Biochem Biophys 122(1):144–152

Klughammer C, Schreiber U (1994) An improved method, using saturating light pulses, for the determination of photosystem I quantum yield via P700+-absorbance changes at 830 nm. Planta 192(2):261–268. https://doi.org/10.1007/bf01089043

Klughammer C, Siebke K, Schreiber U (2013) Continuous ECS-indicated recording of the proton-motive charge flux in leaves. Photosynth Res 117(1–3):471–487. https://doi.org/10.1007/s11120-013-9884-4

Kohzuma K, Cruz JA, Akashi K, Hoshiyasu S, Munekage YN, Yokota A, Kramer DM (2009) The long-term responses of the photosynthetic proton circuit to drought. Plant Cell Environ 32(3):209–219. https://doi.org/10.1111/j.1365-3040.2008.01912.x

Kramer DM, Avenson TJ, Edwards GE (2004) Dynamic flexibility in the light reactions of photosynthesis governed by both electron and proton transfer reactions. Trends Plant Sci 9(7):349–357. https://doi.org/10.1016/j.tplants.2004.05.001

Kreslavski VD, Lyubimov VY, Shabnova NI, Balakhnina TI, Kosobryukhov AA (2009) Heat-induced impairments and recovery of photosynthetic machinery in wheat seedlings. Role of light and prooxidant-antioxidant balance. Physiol Mol Biol Plants 15(2):115–122. https://doi.org/10.1007/s12298-009-0013-y

Kunz HH, Gierth M, Herdean A, Satoh-Cruz M, Kramer DM, Spetea C, Schroeder JI (2014) Plastidial transporters KEA1, -2, and -3 are essential for chloroplast osmoregulation, integrity, and pH regulation in Arabidopsis. Proc Natl Acad Sci U S A 111(20):7480–7485. https://doi.org/10.1073/pnas.1323899111

Law RD, Crafts-Brandner SJ (1999) Inhibition and acclimation of photosynthesis to heat stress is closely correlated with activation of ribulose-1,5-bisphosphate carboxylase/oxygenase. Plant Physiol 120(1):173–182. https://doi.org/10.1104/pp.120.1.173

Lemaire SD, Michelet L, Zaffagnini M, Massot V, Issakidis-Bourguet E (2007) Thioredoxins in chloroplasts. Curr Genet 51(6):343–365. https://doi.org/10.1007/s00294-007-0128-z

Mamedov M, Hayashi H, Murata N (1993) Effects of glycinebetaine and unsaturation of membrane lipids on heat stability of photosynthetic electron-transport and phosphorylation reactions in Synechocystis PCC6803. Biochim Biophys Acta Bioenerg 1142(1–2):1–5

Mao H, Chen M, Su Y, Wu N, Yuan M, Yuan S, Brestic M, Zivcak M, Zhang H, Chen Y (2018) Comparison on photosynthesis and antioxidant defense systems in wheat with different ploidy levels and octoploid triticale. Int J Mol Sci 19(10):3006. https://doi.org/10.3390/ijms19103006

Meyer Y, Belin C, Delorme-Hinoux V, Reichheld J-P, Riondet C (2012) Thioredoxin and glutaredoxin systems in plants: molecular mechanisms, crosstalks, and functional significance. Antioxid Redox Signal 17(8):1124–1160. https://doi.org/10.1089/ars.2011.4327

Miyake C (2020) Molecular mechanism of oxidation of P700 and suppression of ROS production in photosystem I in response to electron-sink limitations in C3 plants. Antioxidants (Basel). https://doi.org/10.3390/antiox9030230

Nellaepalli S, Mekala NR, Zsiros O, Mohanty P, Subramanyam R (2011) Moderate heat stress induces state transitions in *Arabidopsis thaliana*. Biochim Biophys Acta 1807(9):1177–1184. https://doi.org/10.1016/j.bbabio.2011.05.016

Olsen KM, Nygren J, Shad N, Kvarnheden A, Westerbergh A (2015) Variation in susceptibility to wheat dwarf virus among wild and domesticated wheat. PLoS ONE 10(4):e0121580. https://doi.org/10.1371/journal.pone.0121580

Perdomo JA, Carmo-Silva E, Hermida-Carrera C, Flexas J, Galmes J (2016) Acclimation of biochemical and diffusive components of photosynthesis in rice, wheat, and maize to heat and water deficit: implications for modeling photosynthesis. Front Plant Sci 7:1719. https://doi.org/10.3389/fpls.2016.01719

Pšidová E, Živčák M, Stojnić C, Orlović S, Gömöry D, Kučerová J, Ditmarová L, Střelcová D, Brestič M, Kalaji HM (2018) Altitude of origin influences the responses of PSII photochemistry to heat waves in European beech (*Fagus sylvatica* L.). Environ Exp Bot 152:97–106

Ruban AV (2016) Nonphotochemical chlorophyll fluorescence quenching: mechanism and effectiveness in protecting plants from photodamage. Plant Physiol 170(4):1903–1916. https://doi.org/10.1104/pp.15.01935

Sacksteder CA, Kanazawa A, Jacoby ME, Kramer DM (2000) The proton to electron stoichiometry of steady-state photosynthesis in living plants: a proton-pumping Q cycle is continuously engaged. Proc Natl Acad Sci 97(26):14283–14288. https://doi.org/10.1073/pnas.97.26.14283

Salvucci ME, Crafts-Brandner SJ (2004) Relationship between the heat tolerance of photosynthesis and the thermal stability of rubisco activase in plants from contrasting thermal environments. Plant Physiol 134(4):1460–1470. https://doi.org/10.1104/pp.103.038323

Sharkey TD (2005) Effects of moderate heat stress on photosynthesis: importance of thylakoid reactions, rubisco deactivation, reactive oxygen species, and thermotolerance provided by isoprene. Plant Cell Environ 28(3):269–277

Shikanai T, Munekage Y, Kimura K (2002) Regulation of proton-to-electron stoichiometry in photosynthetic electron transport: physiological function in photoprotection. J Plant Res 115(1):3–10. https://doi.org/10.1007/s102650200001

Shimakawa G, Miyake C (2018) Oxidation of P700 ensures robust photosynthesis. Front Plant Sci 9:1617. https://doi.org/10.3389/fpls.2018.01617

Shimakawa G, Miyake C (2019) What quantity of photosystem I is optimum for safe photosynthesis? Plant Physiol 179(4):1479–1485. https://doi.org/10.1104/pp.18.01493

Schneider A, Steinberger I, Herdean A, Gandini C, Eisenhut M, Kurz S, Morper A, Hoecker N, Ruhle T, Labs M, Flugge UI, Geimer S, Schmidt SB, Husted S, Weber AP, Spetea C, Leister D (2016) The evolutionarily conserved protein photosynthesis affected MUTANT71 Is required for efficient manganese uptake at the thylakoid membrane in Arabidopsis. Plant Cell 28(4):892–910. https://doi.org/10.1105/tpc.15.00812

Schrader SM, Kleinbeck KR, Sharkey TD (2007) Rapid heating of intact leaves reveals initial effects of stromal oxidation on photosynthesis. Plant Cell Environ 30(6):671–678

Schürmann P, Buchanan BB (2008) The ferredoxin/thioredoxin system of oxygenic photosynthesis. Antioxid Redox Signal 10(7):1235–1274. https://doi.org/10.1089/ars.2007.1931

Silim SN, Ryan N, Kubien DS (2010) Temperature responses of photosynthesis and respiration in *Populus balsamifera* L.: acclimation versus adaptation. Photosynth Res 104(1):19–30. https://doi.org/10.1007/s11120-010-9527-y

Singh RP, Prasad PVV, Sunita K, Giri SN, Reddy KR (2007) Influence of high temperature and breeding for heat tolerance in cotton:

a review. Adv Agron 93:313–385. https://doi.org/10.1016/s0065-2113(06)93006-5
Snook LK, Dulloo ME, Jarvis A, Scheldeman X, Kneller M (2011) Crop germplasm diversity: the role of Gene Bank Collections in facilitating adaptation to climate change, pp 495–506.https://doi.org/10.1002/9780470960929.ch34
Stefanov D, Petkova V, Denev ID (2011) Screening for heat tolerance in common bean (*Phaseolus vulgaris* L.) lines and cultivars using JIP-test. Sci Horticult 128(1):1–6. https://doi.org/10.1016/j.scienta.2010.12.003
Takizawa K, Cruz JA, Kanazawa A, Kramer DM (2007a) The thylakoid proton motive force in vivo Quantitative, non-invasive probes, energetics, and regulatory consequences of light-induced pmf. Biochim Biophys Acta 1767(10):1233–1244. https://doi.org/10.1016/j.bbabio.2007.07.006
Takizawa K, Kanazawa A, Kramer DM (2007b) Depletion of stromal Pi induces high 'energy-dependent' antenna exciton quenching (qE) by decreasing proton conductivity at CFO-CF1 ATP synthase. Plant Cell Environ 31(2):235–243. https://doi.org/10.1111/j.1365-3040.2007.01753.x
Tan SL, Yang YJ, Liu T, Zhang SB, Huang W (2020) Responses of photosystem I compared with photosystem II to combination of heat stress and fluctuating light in tobacco leaves. Plant Sci 292:110371. https://doi.org/10.1016/j.plantsci.2019.110371
Vegh B, Marcek T, Karsai I, Janda T, Darko E (2018) Heat acclimation of photosynthesis in wheat genotypes of different origin. S Afr J Bot 117:184–192. https://doi.org/10.1016/j.sajb.2018.05.020
Vinyard DJ, Brudvig GW (2017) Progress toward a molecular mechanism of water oxidation in photosystem II. Annu Rev Phys Chem 68:101–116. https://doi.org/10.1146/annurev-physchem-052516-044820
Vos MH, van Gorkom HJ, van Leeuwen PJ (1991) An electroluminescence study of stabilization reactions in the oxygen-evolving complex of photosystem II. Biochim Biophys Acta 1056(1):27–39
Walker BJ, Kramer DM, Fisher N, Fu X (2020) Flexibility in the energy balancing network of photosynthesis enables safe operation under changing environmental conditions. Plants 9(3):301. https://doi.org/10.3390/plants9030301
Wang C, Yamamoto H, Shikanai T (2015) Role of cyclic electron transport around photosystem I in regulating proton motive force. Biochim Biophys Acta 1847(9):931–938. https://doi.org/10.1016/j.bbabio.2014.11.013
Wang J, Luo M-C, Chen Z, You FM, Wei Y, Zheng Y, Dvorak J (2013) Aegilops tauschiisingle nucleotide polymorphisms shed light on the origins of wheat D-genome genetic diversity and pinpoint the geographic origin of hexaploid wheat. New Phytol 198(3):925–937. https://doi.org/10.1111/nph.12164
Watanabe N, Kobayashi S, Furuta Y (1997) Euphytica 94(3):303–309. https://doi.org/10.1023/a:1002936019332
Weis E (1981) The temperature-sensitivity of dark-inactivation and light-activation of the ribulose-1, 5-bisphosphate carboxylase in spinach chloroplasts. FEBS Lett 129(2):197–200
Wise RR, Olson AJ, Schrader SM, Sharkey TD (2004) Electron transport is the functional limitation of photosynthesis in field-grown Pima cotton plants at high temperature. Plant Cell Environ 27(6):717–724
Witt H (1971) Coupling of quanta, electrons, fields, ions and phosphorylation in the functional membrane of photosynthesis. Results by pulse spectroscopic methods. Q Rev Biophys 4(4):365–477
Wolosiuk RA, Buchanan BB (1977) Thioredoxin and glutathione regulate photosynthesis in chloroplasts. Nature 266(5602):565–567. https://doi.org/10.1038/266565a0
Xu S, Li J, Zhang X, Wei H, Cui L (2006) Effects of heat acclimation pretreatment on changes of membrane lipid peroxidation, antioxidant metabolites, and ultrastructure of chloroplasts in two cool-season turfgrass species under heat stress. Environ Exp Bot 56(3):274–285. https://doi.org/10.1016/j.envexpbot.2005.03.002
Yamori W, Makino A, Shikanai T (2016) A physiological role of cyclic electron transport around photosystem I in sustaining photosynthesis under fluctuating light in rice. Sci Rep 6(1). https://doi.org/10.1038/srep20147
Zhang R, Sharkey TD (2009) Photosynthetic electron transport and proton flux under moderate heat stress. Photosynth Res 100(1):29–43. https://doi.org/10.1007/s11120-009-9420-8
Zivcak M, Kalaji HM, Shao HB, Olsovska K, Brestic M (2014) Photosynthetic proton and electron transport in wheat leaves under prolonged moderate drought stress. J Photochem Photobiol B 137:107–115. https://doi.org/10.1016/j.jphotobiol.2014.01.007
Zivcak M, Brestic M, Kunderlikova K, Sytar O, Allakhverdiev SI (2015) Repetitive light pulse-induced photoinhibition of photosystem I severely affects CO_2 assimilation and photoprotection in wheat leaves. Photosynth Res 126(2–3):449–463. https://doi.org/10.1007/s11120-015-0121-1